Mechanism of the Initial Phenomena of Defluidization Caused by Switching Fluidizing Gases

Takami Kai, Yuki Hirano, Tsutomu Nakazato and Kei Mizuta

Department of Chemical Engineering, Kagoshima University, 1-21-40 Korimoto, Kagoshima-shi, Kagoshima 890-0065, Japan

Keywords: Fluidized Bed, Gas Switching, Defluidization, Packed Bed, Graham's Law

In a fluidized bed, particle agglomeration and channeling have been observed when the fluidizing gas is switched from lower to higher density. This defluidization is a transient phenomenon, and fluidization is restored after several minutes. In this paper, we assume this behavior can be explained by non-equimolar diffusion, which causes pressure gradients in the bed and subsequently leads to viscous flow. To verify this assumption, pressure changes were measured for several binary diffusion systems in a packed bed. After the packed bed was filled with a gas, another gas was supplied to the bed's outer surface to replace the first gas. These gases were exchanged by diffusion, and the pressure at the closed end of the column either increased or decreased due to differences in the gases' molecular weights. The pressure changes were compared with pressure changes calculated from a model based on both an unsteady-state diffusion equation and the Kozeny-Carman equation. The measured pressure changes in the packed beds could be correlated with the calculated values without any adjustable parameters. In a fluidized bed, after the gas switched from lower to higher density, differences in diffusion rates due to the gases' various molecular weights caused a net molecular flow from the emulsion phase to the bubble phase. This flow caused a decrease in gas velocity in the emulsion phase and a contraction of the emulsion phase; channeling and defluidization were then observed.

Introduction

When the fluidizing gas is switched from a lower to a higher density gas, particle agglomeration, channeling, and defluidization occur in the fluidized catalyst bed. These poor fluidization phenomena are transient, and fluidization is restored after several minutes. In contrast, these phenomena do not occur when the gas is switched from higher to lower density. These phenomena were first reported by Rietema and Hoebink (1977). They stated that gas adsorption in the particles can be ignored because the transient phenomena occur for both porous catalyst particles and glass beads. They proposed two mechanisms to explain the observed behavior.

In the first mechanism, these phenomena are attributed to the change in gas viscosity because this change affects the expansion of the emulsion phase. Rietema and Hoebink (1977) stated that channels form when the viscosity of the second gas is higher than the viscosity of the first gas. Since the voidage of the emulsion phase increases with gas viscosity (Mutsers and Rietema, 1977; Abrahamsen and Geldart, 1980; Kai *et al.*, 1987), the higher viscosity increases the voidage of the emulsion phase, which causes both bed instabilities and the formation of channels.

In the second mechanism, these phenomena are attributed to the mass flow caused by equimolar diffusion. When the fluidizing gas is switched from lower to higher density, the gas in the bubble phase is changed—after several seconds—from lower to higher density. However, since the gas velocity in the emulsion phase is much lower than the gas velocity in the bubble phase, several minutes elapse before the whole gas is replaced in the emulsion phase. Therefore, for several minutes, a situation is maintained in which the gas density in the bubble phase differs from the gas density in the emulsion phases.

To simulate this situation, Rietema and Hoebink (1977) studied the pressure changes in a packed bed. The bed was first filled with a lower density gas, and a higher density gas was then supplied to the open end of the bed. The experiment showed that the pressure decreased at the closed end. Rietema and Hoebink explained this decrease as follows: when a higher density gas and a lower density gas are exchanged via equimolar counter diffusion, the net molar flux is zero. However, the net mass flow toward the particle bed increased. Dividing the net mass flow by the gas density yields the volumetric flow, and a pressure gradient in the opposite direction is required, as per Darcy's law. Consequently, because of this pressure gradient, the emulsion phase is compressed.

It is not clear how equimolar gas exchange could cause a pressure gradient in the bed. According to the ideal gas law, pressure is proportional to the number of molecules at constant volume and temperature. Kai and Takahashi (1997) performed packed-bed experiments for various gas combinations and found that the pressure change was inversely proportional to the square of the particle size. In addition, the pressure change could be correlated with the difference

Received on September 25, 2013; accepted on October 25, 2013
DOI: 10.1252/jcej.13we246
Correspondence concerning this article should be addressed to T. Kai (E-mail address: t.kai@cen.kagoshima-u.ac.jp).

Copyright © 2014 The Society of Chemical Engineers, Japan

between the reciprocals of the square roots of the gases' molecular weights. To explain these observations, another mechanism was proposed based on non-equimolar diffusion and viscous flow.

In a binary mixture, if the rates of diffusion caused by the two species' molecular movement are not identical, a pressure gradient forms at constant volume. To maintain an isobaric-isothermal system, bulk motion of the mixture should occur (Reid *et al.*, 1977). We assume that equimolar diffusion results from both diffusion and bulk flow in free space. However, when the specific surface area of the flow channel is large, the pressure gradient is not immediately canceled due to viscous resistance. Consequently, a pressure decrease or increase will be observed in the packed bed.

To investigate the mechanism of the development of defluidization, images of this transient phenomenon were captured using a video camera and visualized using digital image conversion (Kai *et al.*, 2013). Gray-scale images were obtained via backlight transmitted through the emulsion phase in a two-dimensional fluidized bed. The gray-scale images were converted to color images using a color gradation based on digital image conversion. The bubble phase, the emulsion phase, and the defluidized region were represented by blue, yellowish green, and red, respectively.

Figure 1 shows the time series of colored images after the gas was switched from He to Ar. The superficial gas velocity of the second gas, Ar, was 0.042 m s^{-1}. Some low-voidage spots formed at the bottom immediately after the gases were switched. In addition, the image at 0.5 s shows that the voidage contracted in the internal area in the emulsion phase, while the voidage did not decrease in the interface area in the emulsion phase.

The mechanism of the development of the defluidized area has already been reported in a previous paper (Kai *et al.*, 2013). In this study, we consider the cause of the initial contraction in the emulsion phase. According to the assumption described above, the net molar flux through the emulsion phase is influenced by a difference in the two species' diffusion rates. As a result, the gas velocity in the emulsion phase decreases, and the gas drag force becomes too small to balance the gravitational and buoyancy forces acting on the particles. This imbalance causes initial local agglomeration in the emulsion phase.

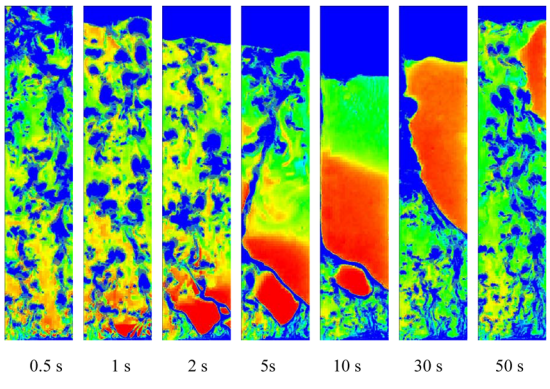


Fig. 1 Change in voidage distribution in a fluidized bed after the fluidizing gas is switched from He to Ar

The effects of gas adsorption on defluidization have been reported (Kai *et al.*, 1998; Reichhold *et al.*, 2002; Reichhold *et al.*, 2006). When the adsorptivity of the second gas is higher than the adsorptivity of the first gas, the gas velocity in the emulsion phase decreases, and transient defluidization is more prominent. Experiments have shown that the gas flow rate at the outlet substantially decreases when the fluidizing gas is switched from He to CO_2 (Reichhold *et al.*, 2006). The influence of gas adsorption is significant for porous particles. A different mechanism for the progression of defluidization was observed when the second gas was adsorptive. However, the effects of gas adsorption are not within the scope of this paper.

Gases are switched during startup and shutdown of a reactor. During an operational startup, temporary defluidization has been observed when the fluidizing gas was changed from an inert to a reactant gas (Reichhold *et al.*, 2002; Reichhold *et al.*, 2006). If a lower density gas is produced by reactions (such as disproportionation reactions), continuous poor fluidization will likely occur. Therefore, from an industrial perspective, it is important to investigate this phenomenon. To verify the proposed mechanism (that the initial contraction in the emulsion phase is induced by non-equimolar diffusion in the binary mixture of gases), we measured pressure changes in a packed bed. The data were compared with calculations based on the unsteady-state diffusion equation and the Kozeny–Carman equation.

1. Experimental

In this study, pressure changes caused by the diffusion of two components were measured in a packed bed. The experimental method was fundamentally identical to the method reported by Rietema and Hoebink (1977). The experimental apparatus in the present study is shown in **Figure 2**. The bed was contained in a horizontal column with an inner diameter of 0.011 m. The column and valves were made of stainless steel. The column was wrapped with a heat-insulating sheet to reduce the effects of fluctuations in room temperature. We packed glass beads in the column to ensure the effects of gas adsorption could be ignored. The length of the bed was varied from 100 to 400 mm. The average sizes of glass beads were 62.4, 76.2, 116, and 163 μm.

Fed from valve A, the bed was first filled with gas A. The

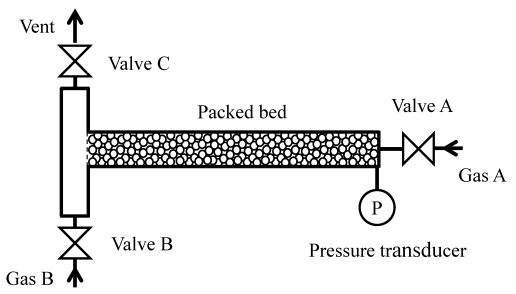


Fig. 2 Experimental apparatus for gas diffusion in a packed bed

other side of the column was open to the atmosphere when valve C was open. Therefore, after valve A was closed and the flow of gas A was stopped, the pressure at this point was atmospheric. Valve B was then opened, and gas B was introduced into the column to sweep the bed surface. A portion of gas B diffused into the bed, and gas A was replaced with gas B. The change in the pressure at the closed end of the bed was measured using a pressure transducer. The signals from the transducer were stored on a logger and analyzed by a computer. The same procedure was repeated under the same conditions, and average values were calculated from ten runs. The six different gases were as follows: H_2, He, N_2, Ar, Ne, and CO_2.

2. Model Equations

Gas transport in a porous material has been extensively studied for porous solid catalysts and membranes. In a porous material, bulk flow arises due to a pressure gradient and is considered in the context of Darcy's law (Altevogt *et al.*, 2003; Suwanwarangkul *et al.*, 2003; Fen and Abriola, 2004; Pisani, 2008; Solsvik and Jakobsen, 2011). The unsteady equation that includes diffusion and bulk flow is

$$\varepsilon \frac{\partial C_i}{\partial t} = \frac{\partial}{\partial z}\left(\frac{\varepsilon}{\tau} D_i \frac{\partial C_i}{\partial z} \right) - \frac{\partial (uC_i)}{\partial z} \tag{1}$$

where u is the bulk flow rate and is described by the Darcy equation. In this study, the Kozeny–Carman equation was used for the bulk flow in a packed bed:

$$u = \frac{d_p^2}{K\mu} \frac{\varepsilon^3}{(1-\varepsilon)^2} \frac{\mathrm{d}P}{\mathrm{d}z} \tag{2}$$

In this study, for each particle size, the value of K in Eq. (2) was obtained from the relationship between gas velocity and pressure drop.

For a binary mixture of A and B, the diffusion coefficient D_i in Eq. (1) is usually the mutual diffusion coefficient of A and B. When the channel size is below the mean free path of the gas molecules, Knudsen diffusion becomes important. The Knudsen diffusion coefficient is inversely proportional to the square root of the molecular weight of each gas. However, the voids formed by the glass beads provide a sizable space for diffusing molecules, and thus Knudsen diffusion is neglected in this study. When a mutual diffusion coefficient is used for a binary system under isothermal-isobaric conditions, equimolar exchange occurs, and a pressure distribution does not exist.

However, experiments show that pressure distribution is generated in the bed, which indicates that non-equimolar gas exchange must also occur in the bed. To explain this phenomenon, we used a diffusion coefficient that depends on the average molecular velocity for each component (instead of the mutual diffusion coefficient for a binary gas mixture). In addition, viscous flow was assumed to be induced by the pressure difference caused by non-equimolar diffusion. Since the channel size was much larger than the molecular mean free path, the continuum assumption was used to describe viscous flow in this study. However, the channel size is not so large that the effect of wall shear stress on the bulk flow rate can be neglected, and the pressure gradient cannot be immediately canceled. This is presumed to be the mechanism for generating the pressure changes observed in a packed bed.

To obtain the diffusion coefficient of component A in a binary mixture, we used the basic equation for self-diffusion coefficients derived from the kinetic theory of dilute gases,

$$D_{AA} = \frac{3}{8} \frac{1}{\rho \sigma_A^2} \left(\frac{kT}{\pi m_A} \right)^{1/2} \tag{3}$$

where ρ is the number density, σ_A is the molecular diameter of molecule A, k is the Boltzmann constant, and m_A is the mass of molecule A.

It is easily recognized that the diffusion coefficient of A in gas A (the self-diffusion coefficient) differs from the diffusion coefficient in B because the diffusion rate depends not only on the average molecular speed but also on the mean free path, which is dominated by collisions with other molecules. Therefore, the diffusion rate of A in a binary mixture is influenced by the composition of the mixture:

$$D_{Am} = \frac{3}{8} \frac{1}{\rho \sigma_{Am}^2} \left(\frac{kT}{\pi m_A} \right)^{1/2} \tag{4}$$

When component A diffuses in a binary mixture of A and B, the average molecular size is estimated from collisions between A and A and between A and B, which is then weighted by the mole fraction of each component:

$$\sigma_{Am} = (0.5 + 0.5 y_A)\sigma_A + 0.5 y_B (0.5\sigma_A + 0.5\sigma_B) \tag{5}$$

The value of the mixture's gas viscosity was calculated from averages involving the mole fractions and viscosities of the pure components using Wilke's method (Wilke, 1950), which provides a reliable estimate for the viscosity of a binary gas mixture (Dutt *et al.*, 1995):

$$\mu_m = \frac{y_A \mu_A}{y_A + y_B \phi_{AB}} + \frac{y_B \mu_B}{y_B + y_A \phi_{BA}} \tag{6}$$

$$\phi_{AB} = \frac{[1 + (\mu_A / \mu_B)^{1/2} (M_B / M_A)^{1/4}]^2}{[8(1 + M_A / M_B)]^{1/2}} \tag{7}$$

$$\phi_{BA} = \phi_{AB} \frac{\mu_B M_A}{\mu_A M_B} \tag{8}$$

The tortuosity factor, τ, in Eq. (1) was obtained from the correlation proposed by Boudreau (1996):

$$\tau = \sqrt{1 - \ln(\varepsilon^2)} \tag{9}$$

3. Results

3.1 Change in pressure

Temporal pressure evolution for the N_2/H_2 and H_2/N_2 systems is shown in **Figure 3** when the bed length was 0.1 m

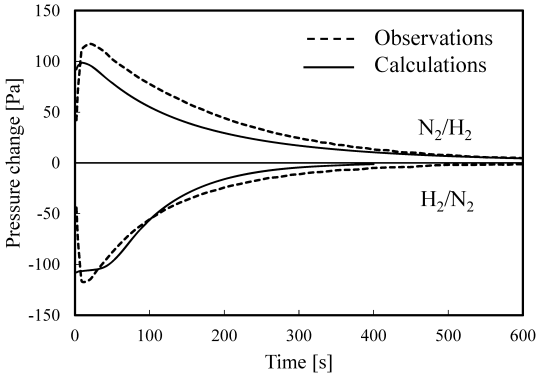


Fig. 3 Observed pressure changes with time for N_2/H_2 and H_2/N_2 systems ($d_p = 62.4\,\mu m$; $L = 0.10\,m$)

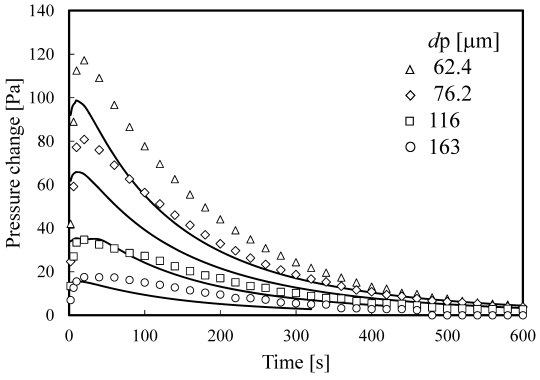


Fig. 4 Effect of particle size on pressure changes for the N_2/H_2 system ($L = 0.10\,m$)

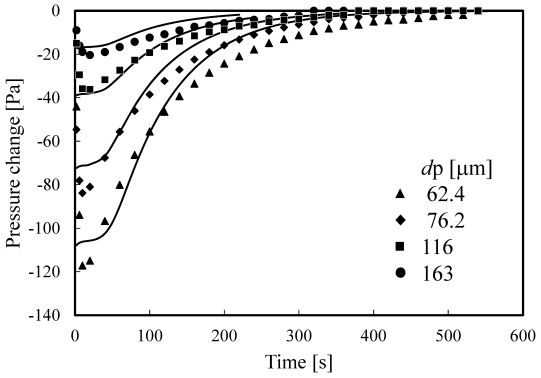


Fig. 5 Effect of particle size on pressure changes for the H_2/N_2 system ($L = 0.10\,m$)

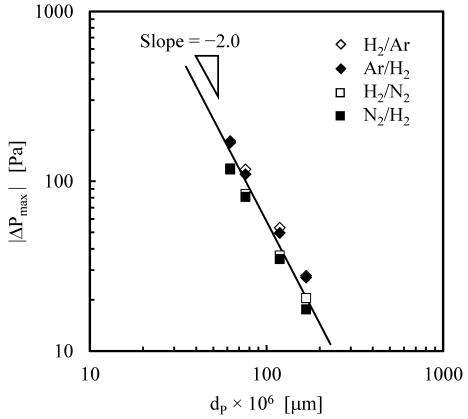


Fig. 6 Effect of particle size on maximum pressure change

and the particle size was 62.4 μm. The dotted lines show the observed values, and the solid lines show the calculated values. These experimental and calculated results are in good agreement.

When N_2 was gas A and H_2 was gas B, the pressure increased immediately after sweeping started. After the pressure peaked at 19 s, the pressure gradually decreased until it reached atmospheric pressure after 900 s. Because the molar flux of H_2 entering the bed was larger than the molar flux of N_2 escaping from the bed, the pressure in the bed increased above atmospheric pressure. However, the viscous flow induced by the pressure gradient moved molecules out of the bed. When the pressure was at maximum, the net molar flux due to diffusion was equal to the molar flux due to the viscous flow, but these two fluxes operated in opposite directions.

When H_2 was gas A and N_2 was gas B, the pressure immediately decreased and reached its minimum value at 13 s. In this case, the molar flux of H_2 escaping from the bed was larger than the molar flux of N_2 entering the bed. Therefore, the pressure curves for the H_2/N_2 and N_2/H_2 systems are almost symmetric along the time axis.

3.2 Effects of particle size

Figures 4 and **5** show the relationship between particle size and the pressure's extreme point. In both cases, the absolute value of the pressure at the extreme point increased with decreasing particle diameter. The recovery time for the pressure to return to atmospheric pressure was not influenced by particle size, but the time to recover was somewhat shorter when the molecular weight was smaller for gas A than for gas B. These tendencies were well predicted by the proposed model, as shown by the solid lines in these figures.

Figure 6 shows the relationship between particle size and the absolute values of the experimentally observed pressure at the extreme point. The slope of the line in this figure is −2.0 and the pressure change is inversely proportional to the square of the particle size, as reported in a previous study (Kai and Takahashi, 1997).

Now let us estimate the pressure at the extreme point. After we start supplying the sweep gas, diffusion of gases A and B begins in a diffusion layer near the bed surface. The total molar flux in this layer is

$$N_D = -D_{AB}\frac{dC_A}{dz} + D_{BA}\frac{dC_B}{dz} \tag{10}$$

Because the bed was initially filled with gas A, whose concentration outside the bed was 0, the diffusion layer during the initial stage was thin. Assuming the thickness of the diffusion layer is Δz, Eq. (10) can be written as:

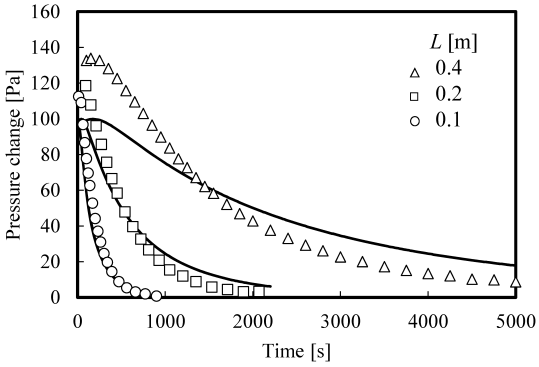


Fig. 7 Effect of bed length on pressure changes for the N_2/H_2 system ($d_p = 62.4\,\mu m$)

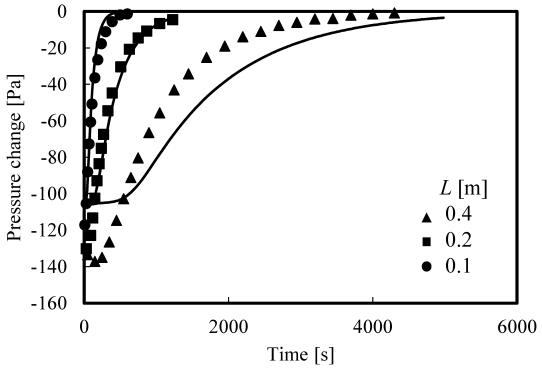


Fig. 8 Effect of bed length on pressure changes for the H_2/N_2 system ($d_p = 62.4\,\mu m$)

$$N_D = (-D_{AB} + D_{BA})\frac{C_0}{\Delta z} \tag{11}$$

However, the viscous flow rate is proportional to the pressure gradient in the diffusion layer:

$$N_B = C_0 u = \frac{C_0 d_p^2}{K\mu}\frac{\varepsilon^3}{(1-\varepsilon)^2}\frac{\Delta P}{\Delta z} \tag{12}$$

When the molar fluxes due to both diffusion and viscous flow are balanced, the pressure difference is

$$\Delta P = \frac{K\mu(1-\varepsilon)^2}{d_p^2\varepsilon^3}(-D_{AB} + D_{BA}) \tag{13}$$

This equation indicates that the pressure at the extreme point is inversely proportional to the square of the particle size. In addition, this pressure is proportional to the difference between the diffusion coefficients of A and B. Because the diffusion coefficient is inversely proportional to the square root of the molecular weight (see Eqs. (3) and (4)), Eq. (13) can explain the observation in a previous paper (Kai and Takahashi, 1997) that the pressure change could be correlated with both the viscosity and the difference between the reciprocals of the square roots of the molecular weights.

3.3 Effects of bed length

Figures 7 and **8** show the effects of bed length on the pressure changes in the H_2/N_2 and N_2/H_2 systems. The maximum and minimum pressure changes were not influenced by bed length, while the time for pressure's recovery was strongly influenced. The recovery time increased with bed length. Using the proposed model (solid lines), this tendency is also well predicted by the calculation.

3.4 Effects of gas type

The extreme values of pressure were also influenced by the combination of gases. When He was gas A, pressure changes increased with gas B in the order $Ne > Ar > CO_2$, N_2, as shown in **Figure 9**. This sequence means that pressure's extreme values were not in the order of the differences between the reciprocals of the square roots of the molecular weights of each gas. This finding results because gas viscosity also affected pressure changes, as shown in Eq. (13). The viscosities of these gases are ordered as $Ne > Ar > N_2 > CO_2$, as shown in **Table 1**. When the viscosity was large, the viscous flow rate was small, and the time necessary to cancel the pressure gradient was long.

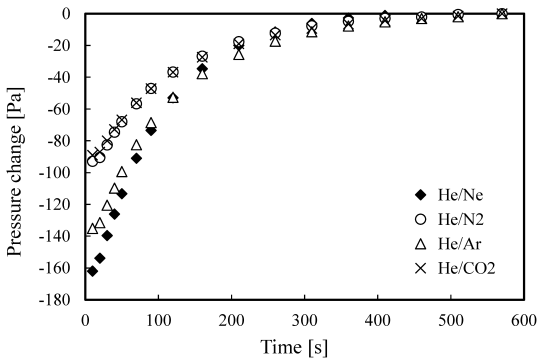


Fig. 9 Observed pressure changes with time for various gas systems ($d_p = 62.4\,\mu m$; $L = 0.10\,m$)

Table 1 Gas properties and maximum pressure changes for the gas combinations shown in Figure 9

Gas	He	Ne	N_2	Ar	CO_2
M [g mol^{-1}]	4.0	20.2	28.0	39.9	44.0
$\mu \times 10^5$ [Pa s]	1.96	3.10	1.78	2.22	1.47
ΔP_{max} [Pa]	—	−161	−92	−135	−89

Figure 10 compares observations and calculations for the pressures at the extreme points for various gas combinations. The bed length was 0.10 m, and the average particle size was 62.4 μm. In this figure, the slope of the line is not unity. The model was very simple and did not involve any adjustable parameters; therefore, the agreement is reasonable. If a factor of 1.14 is introduced into the calculated values, better agreement between the observations and the calculations is obtained.

4. Discussion

Non-equimolar diffusion through a porous material was reported by Graham (1833) about 180 years ago. He con-

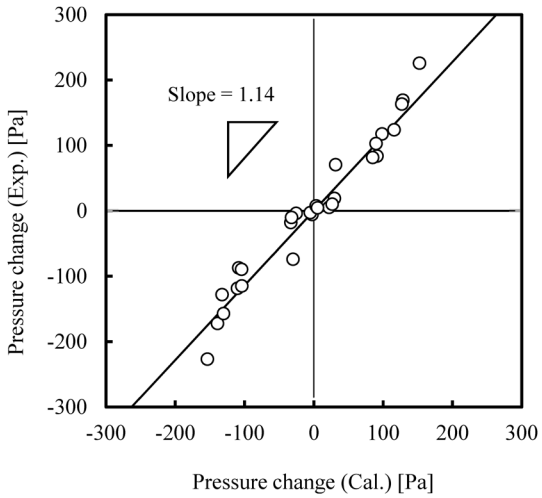


Fig. 10 Comparison of calculated and experimental maximum pressure changes ($d_p = 62.4\,\mu m$; $L = 0.10\,m$)

cluded that the molar fluxes were inversely proportional to the square roots of the molecular weights. Experimental studies obeyed this relationship for isobaric counterdiffusion (Remick and Geankoplis, 1973; Knaff and Schlünder, 1985). Conversely, pressure change was observed for isovolumetric counterdiffusion (Asaeda *et al.*, 1981; Veldsink *et al.*, 1994; Soukup *et al.*, 2008). Although models have also been proposed to explain these results, they involve Knudsen diffusivity, which depends on molecular weight. The model proposed in this study can also predict the observations of Graham without considering Knudsen diffusivity. Although the model used in this study was quite simple, the experimentally observed phenomena were well described.

The pressure changes observed in the packed-bed experiments appear to result from non-equimolar gas exchange at constant volume. In the case of fluidized beds, because a small amount of gas flows in the emulsion phase, non-equimolar diffusion will affect not only the pressure in the emulsion phase but also the gas velocity in the emulsion phase. Changes in gas velocity in the emulsion phase were simulated by the model proposed in this study. In the calculation, the voidage was assumed to be 0.45, the average particle size was 62.4 μm, and the horizontal depth of the area considered in the calculation was 20 mm. In addition, the pressure decrease in the emulsion phase at the closed end of the bed was assumed to be below 5 Pa. The bed was initially filled with H_2, and H_2 was then replaced by N_2.

Figure 11 shows the distribution of relative gas velocities in the particle bed. The gas velocity at 4 mm inside the interface decreased to 93% after 0.1 s. The gas velocity in the area excluding the particle bed's interface region was below 90% after 0.5 s. These results agree with observations of voidage in the emulsion phase described in the introduction: the voidage contracts in the internal area in the emulsion phase, but the voidage does not decrease in the emulsion phase near the bubble phase. **Figure 12** shows in detail the change in bed voidage at the bottom region obtained by the proposed method (Kai *et al.*, 2013). The size of this area was

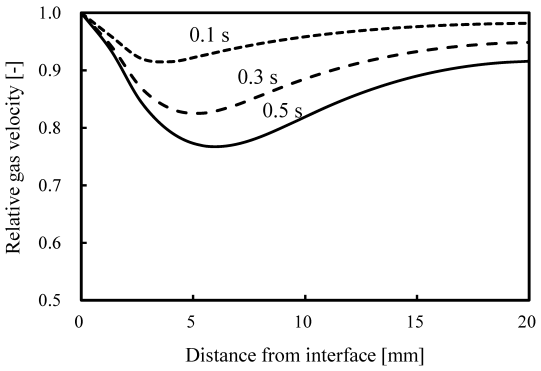


Fig. 11 Gas velocity distribution calculated from the model when $d_p = 62.4\,\mu m$

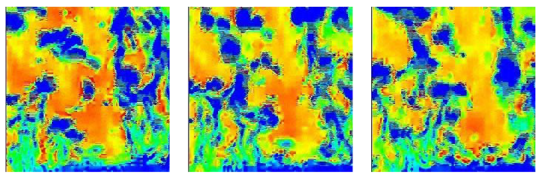


Fig. 12 Change in the emulsion phase voidage at the bottom of the bed after gas switching from He to Ar

80×80 mm. It can be seen that voidage contraction occurred in the internal area in the emulsion phase. This contraction is the beginning of the defluidization that subsequently occurs.

When the particle size is 300 μm, the calculation shows that change in gas velocity is insignificant. Since the particle size is large and the particle bed's resistance to viscous flow is small, pressure gradients due to non-equimolar diffusion are simultaneously canceled. Consequently, when the particle size is large, equimolar gas exchange arises between the emulsion and the bubble phases.

Conclusion

A model using the unsteady-state diffusion equation and the Kozeny–Carman equation has been proposed to study transient defluidization that occurs after the fluidizing gas is switched to another gas. Experimental pressure changes for a binary diffusion system in a packed bed could be well predicted by the model without the inclusion of any adjustable parameters. This result confirms that the defluidization is caused by non-equimolar gas exchange between the bubble and the emulsion phases.

For the gas exchange between the bubble and the emulsion phases in a fluidized bed, non-equimolar gas exchange through the bubble interface induces a pressure gradient. However, when the particle size is small (as for fluidized catalysts), the pressure gradient cannot be immediately canceled by viscous resistance, and equimolar gas exchange cannot be established. In addition to pressure, non-equimolar gas exchange should also affect gas velocity in the emulsion phase. Therefore, gas velocity in the emulsion phase

decreases below the minimum fluidization velocity, the emulsion phase contracts, and finally defluidization occurs.

Nomenclature

C	=	concentration	$[\mathrm{mol\,m^{-3}}]$
D	=	diffusion coefficient $[\mathrm{m^2\,s^{-1}}]$	
d_p	=	particle diameter	[m]
K	=	constant in Kozeny–Carman equation	[—]
k	=	Boltzmann constant	$[\mathrm{kg\,m^2\,s^{-2}\,K^{-1}}]$
L	=	length of glass bead bed	[m]
M	=	molecular weight	$[\mathrm{g\,mol^{-1}}]$
m	=	mass of molecule	[kg]
N_D	=	molar flux by diffusion	$[\mathrm{mol\,m^{-2}\,s^{-1}}]$
N_B	=	molar flux by bulk flow	$[\mathrm{mol\,m^{-2}\,s^{-1}}]$
P	=	pressure	[Pa]
T	=	temperature	[K]
t	=	time	[s]
u	=	bulk flow rate	$[\mathrm{m\,s^{-1}}]$
y	=	mole fraction	[—]
z	=	distance from bed surface	[m]
ΔP	=	pressure change	[Pa]
ΔP_{max}	=	maximum pressure change	[Pa]
ε	=	voidage of packed bed	[—]
μ	=	gas viscosity	[Pa s]
ρ	=	number density	$[\mathrm{m^{-3}}]$
σ	=	molecular diameter	[m]
τ	=	tortuosity of packed bed	[—]
ϕ	=	mixture viscosity parameter in Eqs. (6)–(8)	[—]

‹Subscripts›

A, B	=	components A, B
i	=	component i
m	=	mixture of A and B

Literature Cited

Abrahamsen, A. R. and D. Geldart; "Behavior of Gas-Fluidized Beds of Fine Powders Part II. Voidage of the Dense Phase in Bubbling Beds," *Powder Technol.*, **26**, 47–55 (1980)

Altevogt, A. S., D. E. Rolston and S. Whitaker; "New Equations for Binary Gas Transport in Porous Media, Part 1: Equation Development," *Adv. Water Resour.*, **26**, 695–715 (2003)

Asaeda, M., J. Watanabe and M. Kitamoto; "Effect of Total Pressure Gradient on Unsteady-State Diffusion Rates of Gases in Porous Media," *J. Chem. Eng. Japan*, **14**, 129–135 (1981)

Boudreau, B. P.; "The Diffusive Tortuosity of Fine-Grained Unlithified Sediments," *Geochim. Cosmochim. Acta*, **60**, 3139–3142 (1996)

Dutt, N. V. K., Y. V. L. R. Kumar and D. H. L. Prasad; "A Simple Generalization of Low-Pressure Viscosity of Gases and Mixtures," *Chem. Eng. J. Biochem. Eng. J.*, **56**, 67–72 (1995)

Fen, C. S. and L. M. Abriola; "A Comparison of Mathematical Model Formulations for Organic Vapor Transport in Porous Media," *Adv. Water Resour.*, **27**, 1005–1016 (2004)

Graham, T.; "On the Law of the Diffusion of Gases," *London-Edinburgh Philos. Mag. J. Sci.*, **2**, 175–190, 269–276, 351–358 (1833)

Kai, T., A. Iwakiri and T. Takahashi; "Emulsion Phase Expansion and Sedimentation Velocity in Fluidized Beds of Fine Particles," *J. Chem. Eng. Japan*, **20**, 282–286 (1987)

Kai, T. and T. Takahashi; "Formation of Particle Agglomerates after Switching Fluidizing Gases," *AIChE J.*, **43**, 357–362 (1997)

Kai, T., T. Kamei and T. Takahashi; "Effect of Gas Adsorption on Defluidization after Switching Fluidizing Gases," *AIChE J.*, **44**, 491–494 (1998)

Kai, T., Y. Tashiro, Y. Hirano and T. Nakazato; "Visualization of Defluidization Phenomena caused by Gas Switching in a Two-Dimensional Fluidized," *Powder Technol.*, **237**, 153–159 (2013)

Knaff, G. and E. U. Schlünder; "Experimental Confirmation of Graham's Law of Diffusion up to Pore Diameters of 2 µm," *Chem. Eng. Process.*, **19**, 167–173 (1985)

Mutsers, S. M. P. and K. Rietema; "The Effect of Interparticle Forces on the Expansion of a Homogeneous Gas-Fluidized Bed," *Powder Technol.*, **18**, 239–248 (1977)

Pisani, L.; "Multi-Component Gas Mixture Diffusion through Porous Media: A 1D Analytical Solution," *Int. J. Heat Mass Transfer*, **51**, 650–660 (2008)

Reichhold, A., G. Friedl, B. Kronberger and H. Hofbauer; "Temporary Defluidization in Fine Powder Fluidised Beds Caused by Changing the Fluidization Gas," *Chem. Eng. Technol.*, **25**, 363–368 (2002)

Reichhold, A., B. Kronberger and G. Friedl; "Temporary Defluidization in Fine Powder Fluidized Beds Caused by Changing the Fluidizing Gas," *Chem. Eng. Sci.*, **61**, 2428–2436 (2006)

Reid, R. C., J. M. Prausnitz and T. K. Sherwood; The Properties of Gases and Liquids, McGraw-Hill Book Co., New York, U.S.A. (1977)

Remick, R. R. and C. J. Geankoplis; "Binary Diffusion of Gases in Capillaries in the Transition Region between Knudsen and Molecular Diffusion," *Ind. Eng. Chem. Fundam.*, **12**, 214–220 (1973)

Rietema, K. and J. Hoebink; "Transient Phenomena in Fluidized Beds when Switching the Fluidizing Agent from One Gas to Another," *Powder Technol.*, **18**, 257–265 (1977)

Solsvik, J. and H. A. Jakobsen; "Modeling of Multicomponent Mass Diffusion in Porous Spherical Pellets: Application to Steam Methane Reforming and Methanol Synthesis," *Chem. Eng. Sci.*, **66**, 1986–2000 (2011)

Soukup, K., P. Schneider and O. Šolcová; "Wicke–Kallenbach and Graham's Diffusion Cells: Limits of Application for Low Surface Area Porous Solids," *Chem. Eng. Sci.*, **63**, 4490–4493 (2008)

Suwanwarangkul, R., E. Croiset, M. W. Fowler, P. L. Douglas, E. Entchev and M. A. Douglas; "Performance Comparison of Fick's, Dusty-Gas and Stefan–Maxwell Models to Predict the Concentration Overpotential of a SOFC Anode," *J. Power Sources*, **122**, 9–18 (2003)

Veldsink, J. W., G. F. Versteeg and W. P. M. van Swaaij; "An Experimental Study of Diffusion and Convection of Multicomponent Gases through Catalytic and Non-Catalytic Membranes," *J. Membr. Sci.*, **92**, 275–291 (1994)

Wilke, C. R.; "A Viscosity Equation for Gas Mixtures," *J. Chem. Phys.*, **18**, 517–519 (1950)